Atmospheric Methane and Nitrous Oxide of the Late Pleistocene from Antarctic Ice Cores

Renato Spahni, *et al.*

Science **310**, 1317 (2005);
DOI: 10.1126/science.1120132

The CO_2 record from the EPICA Dome C ice core reveals that atmospheric CO_2 variations during glacial-interglacial cycles had a notably different character before and after 430 kyr B.P. Before MIS 11, the amplitude of temperature was lower, and the duration of the warm phases has been much longer since then. In spite of these differences, the significant covariation of δD and CO_2 is valid in both periods. Before MIS 11, CO_2 concentrations did not exceed 260 ppmv. This is substantially lower than the maxima of the last four glacial cycles. The lags of CO_2 with respect to the Antarctic temperature over glacial terminations V to VII are 800, 1600, and 2800 years, respectively, which are consistent with earlier observations during the last four glacial cycles.

Our measurements have revealed an unexpected stable climate phase (MIS 15.1) during which the atmospheric CO_2 concentration was 251.5 ± 1.9 ppmv for many millennia (28,000 years, based on the EDC2 time scale), although the duration of MIS 15.1 is uncertain because of possible inaccuracies in the Dome C EDC2 time scale between MIS 12 and 15. However, the roughly 30,000-year duration of MIS 11 (and possibly MIS 15.1) demonstrates that long interglacials with stable conditions are not exceptional. Short interglacials such as the past three therefore are not the rule and hence cannot serve as analogs of the Holocene, as postulated recently (*24*). Examining δD as a function of CO_2, we observe that the slope during the two new glacial cycles compared to the last four cycles is essentially the same. Therefore, the coupling of Antarctic temperature and CO_2 did not change significantly during the last 650 kyear, indicating rather stable coupling between climate and the carbon cycle during the late Pleistocene.

References and Notes

1. L. Augustin *et al.*, (EPICA community members), *Nature* **429**, 623 (2004).
2. J.-M. Barnola, D. Raynaud, Y. S. Korotkevich, C. Lorius, *Nature* **329**, 408 (1987).
3. D. M. Etheridge *et al.*, *J. Geophys. Res.* **101**, 4115 (1996).
4. B. Stauffer *et al.*, *Nature* **392**, 59 (1998).
5. H. Fischer, M. Wahlen, J. Smith, D. Mastroianni, B. Deck, *Science* **283**, 1712 (1999).
6. A. Indermühle *et al.*, *Nature* **398**, 121 (1999).
7. J. R. Petit *et al.*, *Nature* **399**, 429 (1999).
8. A. Indermühle, E. Monnin, B. Stauffer, T. F. Stocker, M. Wahlen, *Geophys. Res. Lett.* **27**, 735 (2000).
9. E. Monnin *et al.*, *Science* **291**, 112 (2001).
10. K. Kawamura *et al.*, *Tellus* **55B**, 126 (2003).
11. E. Monnin *et al.*, *Earth Planet. Sci. Lett.* **224**, 45 (2004).
12. U. Siegenthaler *et al.*, *Tellus* **57B**, 51 (2005).
13. J. Flückiger *et al.*, *Global Biogeochem. Cycles* **16**, 1010 (2002).
14. J. Ahn *et al.*, *J. Geophys. Res.* **109**, 10.1029/2003JD004415 (2004).
15. P. Falkowski *et al.*, *Science* **290**, 291 (2000).
16. Supplementary information concerning methods or assumptions is available on *Science* Online.
17. F. C. Bassinot *et al.*, *Earth Planet. Sci. Lett.* **126**, 91 (1994).
18. J. Jouzel *et al.*, in preparation.
19. L. E. Lisiecki, M. E. Raymo, *Paleoceanography* **20**, 10.1029/2004PA001071 (2005).
20. D. W. Oppo, J. F. McManus, J. L. Cullen, *Science* **279**, 1335 (1998).
21. J. F. McManus, D. W. Oppo, J. L. Cullen, *Science* **283**, 971 (1999).
22. B. P. Flower *et al.*, *Paleoceanography* **15**, 388 (2000).
23. A. Landais *et al.*, *J. Geophys. Res.* **109**, 10.1029/2003JD004193 (2004).
24. W. F. Ruddiman, *Clim. Change* **61**, 261 (2003).
25. F. Joos, S. Gerber, I. C. Prentice, B. L. Otto-Bliesner, P. J. Valdes, *Global Biogeochem. Cycles* **18**, 10.1029/2003GB002156 (2004).
26. R. Spahni *et al.*, *Science* **310**, 1317 (2005).
27. E. W. Wolff *et al*, in preparation.
28. D. Raynaud *et al.*, *Nature* **436**, 39 (2005).
29. V. Masson *et al.*, *Quaternary Res.* **54**, 348 (2000).
30. J. Schwander, B. Stauffer, *Nature* **311**, 45 (1984).
31. J. Schwander *et al.*, *Geophys. Res. Lett.* **28**, 4243 (2001).
32. N. Caillon *et al.*, *Science* **299**, 1728 (2003).
33. J. Jouzel *et al.*, *Nature* **329**, 403 (1987).

34. We thank K. Kawamura and G. Teste for assisting with the CO_2 measurements, L. Lisiecki and M. Raymo for access to the data of (*19*), and R. Spahni and F. Parrenin for fruitful discussions. This work is a contribution to the EPICA, a joint European Science Foundation/European Commission (EC) scientific program funded by the EC and by national contributions from Belgium, Denmark, France, Germany, Italy, Netherlands, Norway, Sweden, Switzerland, and United Kingdom. We acknowledge long-term financial support by the Swiss National Science Foundation, the University of Bern, the Swiss Federal Office of Energy, and EC Project EPICA-MIS. This is EPICA publication no. 133.

Supporting Online Material

www.sciencemag.org/cgi/content/full/310/5752/1313/DC1
Materials and Methods
Figs. S1 and S2
References

13 September 2005; accepted 1 November 2005
10.1126/science.1120130

Atmospheric Methane and Nitrous Oxide of the Late Pleistocene from Antarctic Ice Cores

Renato Spahni,[1] Jérôme Chappellaz,[2] Thomas F. Stocker,[1]* Laetitia Loulergue,[2] Gregor Hausammann,[1] Kenji Kawamura,[1]† Jacqueline Flückiger,[1]‡ Jakob Schwander,[1] Dominique Raynaud,[2] Valérie Masson-Delmotte,[3] Jean Jouzel[3]

The European Project for Ice Coring in Antarctica Dome C ice core enables us to extend existing records of atmospheric methane (CH_4) and nitrous oxide (N_2O) back to 650,000 years before the present. A combined record of CH_4 measured along the Dome C and the Vostok ice cores demonstrates, within the resolution of our measurements, that preindustrial concentrations over Antarctica have not exceeded 773 ± 15 ppbv (parts per billion by volume) during the past 650,000 years. Before 420,000 years ago, when interglacials were cooler, maximum CH_4 concentrations were only about 600 ppbv, similar to lower Holocene values. In contrast, the N_2O record shows maximum concentrations of 278 ± 7 ppbv, slightly higher than early Holocene values.

Earth's climate during the late Pleistocene was characterized by ice age cycles with relatively short warm periods (interglacials) and longer cold periods (glacials) (*1*). The Vostok ice core provided an archive of climate and atmospheric composition over the past four climatic cycles back to marine isotope stage (MIS) 11, about 420 thousand years before the present (420 kyr B.P.) (*2*). That record demonstrated the high correlation of temperature changes with greenhouse gas concentration changes in the atmosphere in the past. The European Project for Ice Coring in Antarctica (EPICA) Dome Concordia (Dome C) ice core (75°06′S, 123°21′E, 3233 m above sea level) provides an ice core archive much longer, spanning eight climatic cycles over the past 740 thousand years (ky) (*3*). It demonstrates that the oldest four interglacials were cooler but lasted longer than the younger interglacials. Such findings raise the question whether the greenhouse gases CH_4 and N_2O behaved differently before MIS 11. Here, we present CH_4 and N_2O records derived from the EPICA Dome C ice cores reaching back to 650 kyr B.P.

[1]Climate and Environmental Physics, Physics Institute, University of Bern, Sidlerstrasse 5, CH-3012 Bern, Switzerland. [2]Laboratoire de Glaciologie et Géophysique de l'Environnement (LGGE, CNRS-UJF), CNRS, 54 Rue Molières, 38402 St. Martin d'Hères, Grenoble, France. [3]Institut Pierre Simon Laplace/Laboratoire des Sciences du Climat et de l'Environnement, CEA-CNRS 1572, CE Saclay, Orme des Merisiers, 91191 Gif-sur-Yvette, France.

*To whom correspondence should be addressed: stocker@climate.unibe.ch
†Present address: Scripps Institution of Oceanography, University of California, San Diego, 9500 Gilman Drive, La Jolla, CA 92093–0244, USA.
‡Present address: Institute of Arctic and Alpine Research, University of Colorado at Boulder, 450 UCB Boulder, Colorado 80309–0450, USA.

Extracting air from bubbles trapped in polar ice enables us to reconstruct directly the past composition of the atmosphere. The records of CH_4 and N_2O over the past thousand years (*4*–*6*), the Holocene (*7*, *8*), the transition from the last glacial maximum (LGM) to the Holocene (*6*, *9*), parts of the last glacial period (*10*–*14*), and the last four glacial-interglacial cycles (*2*, *15*–*17*) have provided important information about environmental changes in response to regional and global climate variations. Variations in the concentration of globally well-mixed atmospheric CH_4 are attributed to variations in the extent and the productivity of natural wetlands, the main natural sources (*18*). Similarly, variations in the atmospheric N_2O burden are thought to be dominated by variations in the global source strength. About two-thirds of the total preanthropogenic N_2O sources are terrestrial soils, and one-third are nitrification and denitrification processes in the ocean (*13*).

We present high-resolution records of CH_4 and N_2O covering MISs 2 to 7 (Fig. 1), to compare with existing records, and MISs 11 to 16 (Fig. 2), to extend the records back to an age of 650 kyr B.P. Measurements were performed along the EPICA Dome C ice cores (EDC96 and EDC99) at 553 and 476 different depth levels for CH_4 and N_2O, respectively, at the University of Bern and at Laboratoire de Glaciologie et Géophysique de l'Environnement (LGGE) (*19*). The mean CH_4 time resolution is 770 years for MISs 2 to 7 and 840 years for MISs 11 to 16. All ages and their uncertainties are based on the EPICA EDC2 gas and ice age scales (*3*). N_2O analyses were performed only at Bern. Their resolution is similar for MISs 2 to 7 (760 years) but lower for MISs 12 to 16 (1110 years). To be consistent with existing Dome C data, offset corrections for both gases and both laboratories have been applied (*19*).

The Dome C N_2O record is disturbed by artifacts in certain depth intervals as in other ice cores (*6*, *13*, *17*, *20*). High scattering of N_2O values is observed in depth intervals with elevated dust concentrations (*19*) (figs. S1 and S2) during parts of the cold periods MISs 2, 4, 6, 12, 14, and 16 (fig. S3). The EPICA Dome C dust record (*19*) is used to define depth intervals where the dust concentration exceeds 300 ppbw (parts per billion by weight). N_2O measurements in these depths are considered to be disturbed by artifacts and excluded from the record (fig. S3). The good agreement of the remaining record with records measured along other ice cores (Fig. 1) with different characteristics in the concentration of chemical impurities (*6*, *13*, *14*, *17*) supports the assumption that this record shows atmospheric concentrations of the past. Although all samples might be contaminated at some level, no outliers are observed during the

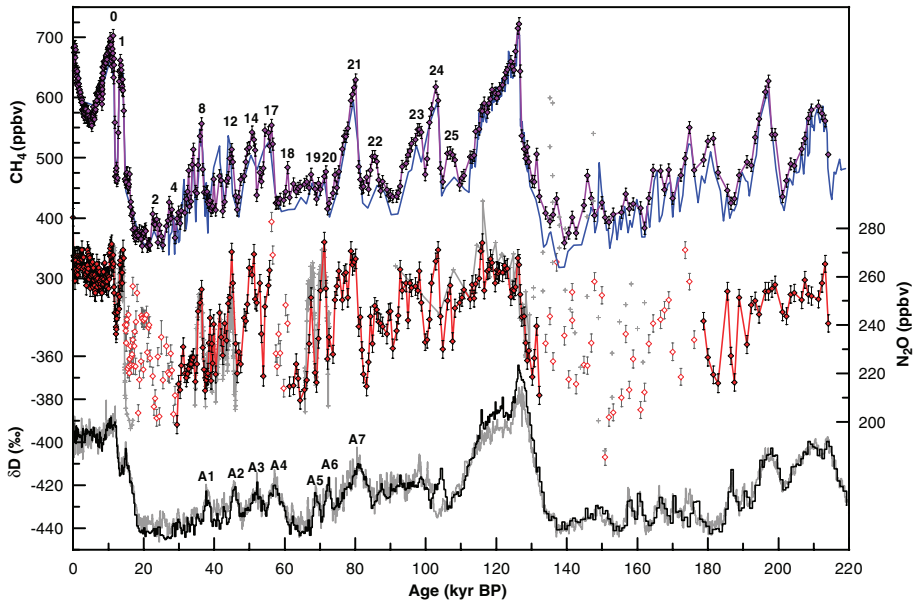

Fig. 1. Dome C CH_4 (purple line), N_2O (red line), and δD (black line) (*3*) records over the past 220 ky. Also shown are Vostok CH_4 data (blue line) (*2*, *15*) and δD data (gray line) (*2*). Vostok δD data were increased by 42‰ for better comparison. The Vostok CH_4 and δD records were individually synchronized to Dome C using wiggle matching (*35*). N_2O artifacts (open red diamonds) are separated from the N_2O record (red filled diamonds) with the aid of the dust record (figs. S1 to S3). Additionally, N_2O records published earlier (gray lines and crosses) (*6*, *13*, *17*), matched by CH_4 to Dome C, are shown for comparison. Error bars represent the 1 SD measurement uncertainty. Dome C CH_4 and N_2O data over the Holocene (*8*), the transition (*9*, *36*), and the LGM (*20*, *36*) are included in this data set. Dome C measurements covering the time period 0 to 40 kyr B.P. (depth interval 99.5 to 783.8 m) were performed along the EDC96 core, whereas older samples are from the EDC99 core. Numbers 0 to 25 above the CH_4 record denote D/O events (*23*), and A1 to A7 denote Antarctic warming events (*37*). Data are plotted on the EDC2 time scale (*3*).

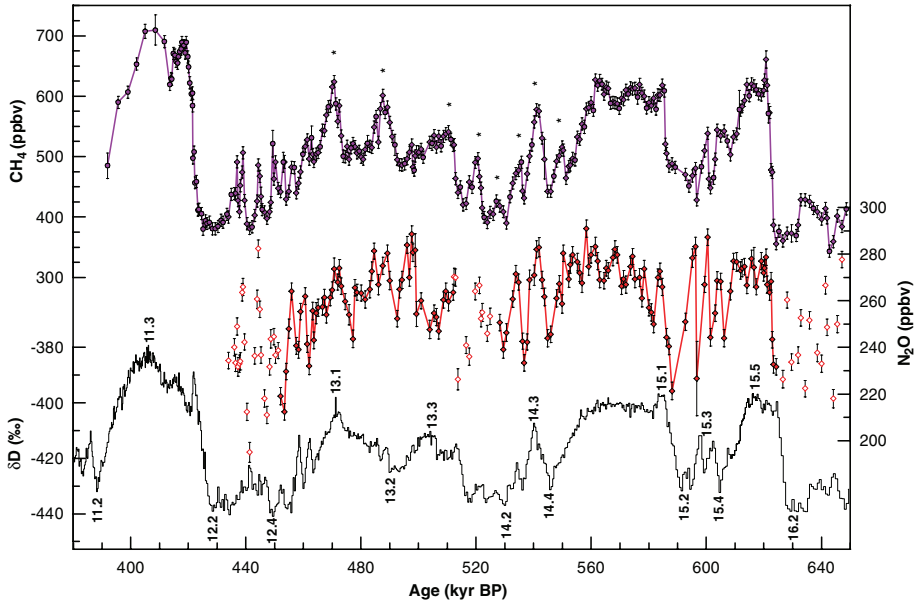

Fig. 2. Dome C CH_4 (purple line) and N_2O (red line) records over the period of MISs 11 to 16, together with high-resolution δD data from Dome C (*24*) (black line). CH_4 measurements performed at Bern are shown as purple diamonds, whereas LGGE measurements are shown as purple circles. N_2O artifacts (red open diamonds) are separated from the N_2O record (red filled diamonds) with the aid of the dust record (figs. S1 to S3). Error bars represent the 1 SD measurement uncertainty. Dome C CH_4 data over termination V (*3*) is included in this data set. Parts of the CH_4 record marked with a star (*) are regular events whose amplitude could be strongly influenced by the precession signal as seen in low-to mid-northern latitude summer insolation. MISs are labeled on the bottom (cold stages) and top (warm stages) of the δD record. Data are shown on the EDC2 time scale (*3*).

highly resolved Holocene. This supports our assumption that other interglacials are also likely free from artifacts.

The Dome C CH_4 data over the last two glacial cycles (Fig. 1) are in good agreement with the Vostok CH_4 record (*15*, *19*), as well as Greenland CH_4 records, when taking into account the interpolar difference (*7*, *21*) and the signal attenuation at low accumulation sites (*22*). The Dome C CH_4 data over the last glacial period confirm the close relation with the 25 Dansgaard/Oeschger (D/O) events as recorded in the North Greenland Ice-Core Project (NGRIP) temperature proxies (*23*). In addition, we find that N_2O also varied during the last glacial period in parallel with the most prominent D/O events (Fig. 1), in agreement with previous results (*6*, *13*, *14*, *16*). N_2O reaches Holocene concentrations of 253 to 272 ppbv (parts per billion by volume) (single values) (*8*) during the maximum of some of these events and during the last interglacial (*14*, *17*). The lowest values found, about 200 ppbv, are similar to those in records published earlier (*13*, *14*). Because the CH_4 and N_2O measurements were performed on the same extracted air samples, a direct comparison without relative time uncertainty is possible between the two gases. The start and end points of single D/O events in CH_4 and N_2O do not necessarily coincide (*13*); e.g., the N_2O concentrations at D/O event 21 start to rise more than 1000 years earlier than CH_4 concentrations. Furthermore, N_2O remains at interglacial values for this specific event, when CH_4 has already dropped to glacial values at the end of the event. The amplitude of some events differs substantially between the two gases as demonstrated by D/O events 19 and 20, also shown in the GRIP record (*13*) (Fig. 1).

The depth interval from 2700 to 3060 m in the EPICA Dome C core permits us to make reconstructions of climate and atmospheric composition for the interval 390 to 650 kyr B.P., most of which precedes the Vostok record (*2*). CH_4 and N_2O measurements performed over this depth interval are shown in Fig. 2, together with high-resolution δD measurements (*24*).

To better characterize warm and cold intervals during the past 650 ky, we refer to "interglacial" as a period during which δD exceeds –403‰ (per mil) (*3*). The use of this definition marks MISs 1, 5.5, 7.3, 7.5, 9.3, and 11.3 as interglacials, which is consistent with the marine records (*1*). In the following, we describe the individual counterparts of the marine stages (*25*) from MISs 16.2 to 11.2.

At 624 kyr B.P., at the end of MIS 16.2, CH_4 falls to a value of 368 ppbv (mean over 7 ky), comparable to the low CH_4 concentration during MIS 6 and MIS 2 in the Dome C record. The increase (termination VII) into MIS 15.5 by about 250 ppbv is smaller than at the younger terminations I, II, IV, and V (*15*). While CH_4 only reaches the mean Holocene (0.3 to 10 kyr B.P.) level of 608 ppbv during MIS 15.1 (600 ppbv, mean over 27 ky) and 15.5 (617 ppbv, mean over 7 ky), the corresponding mean N_2O concentrations of 272 ppbv and 274 ppbv are higher than the Holocene mean (262 ppbv) but similar to early Holocene values. Both records, CH_4 and N_2O, show the distinct separation of MISs 15.1 and 15.5 (Fig. 2) by lower concentrations and three shorter events each during the colder near-glacial periods of MISs 15.2 to 15.4. MIS 15.1 is a surprisingly stable climatic period (1 SD: ± 15 ppbv CH_4, ± 6 ppbv N_2O). Its duration is about 27 ky on the EDC2 age scale. A similar duration is seen in the records of δD (*24*) and CO_2 (*26*); related uncertainties are discussed in (*26*).

In Fig. 3A, δD is plotted together with CO_2 (*26*), CH_4, and N_2O, showing the transition from MISs 14 to 13. During MIS 14, the three gases are closely linked in terms of their timing: Relative maxima (dashed lines) occur at the same time within the data resolution. One of these maxima corresponds to MIS 14.3. CO_2, CH_4, and N_2O seem to lead the δD record and therefore, Antarctic temperature, by about 2000 ± 500 years. However, this could be due to an artifact in the EDC2 time scale, as discussed in Siegenthaler *et al.* (*26*). During MIS 13, the relative CO_2, CH_4, and N_2O maxima are slightly out of phase. In contrast to younger glacial terminations (*2*), the temperatures do not rise directly to a local maximum. Instead, the δD, CO_2, and CH_4 records reveal a transition to the warmest phase (MIS 13.1), which evolves in steps with relapses in between. Nevertheless, sequences of the CO_2 and CH_4 increases to

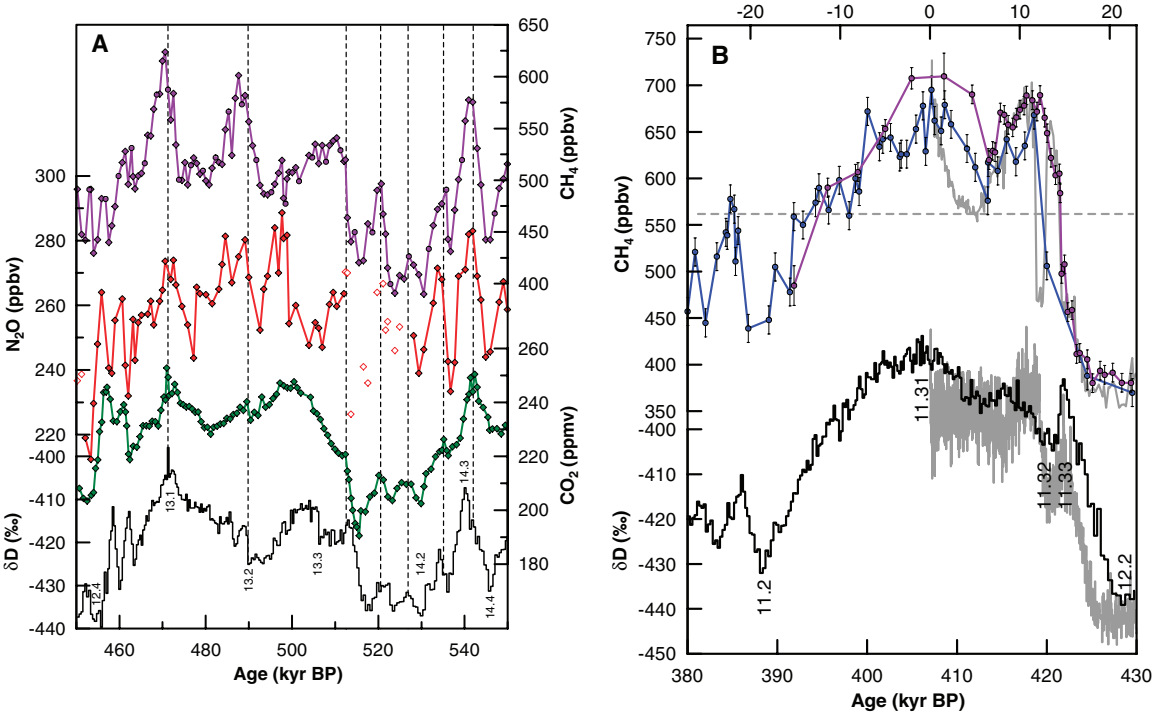

Fig. 3. (**A**) Dome C CO_2 (*26*) (green line), CH_4 (purple line), and N_2O (red line) records over the period of MISs 13 to 14 as shown in Fig. 2, together with high-resolution δD data from Dome C (*24*) (black line). Vertical dashed lines highlight the coincidence of local CO_2, CH_4, and N_2O maxima. Data are plotted on the EDC2 time scale (*3*). (**B**) CH_4 records from Dome C (purple line) and Vostok (*15*, *30*) (blue line), together with high-resolution δD data from Dome C (*24*) (black line) covering MIS 11 (labeled at the bottom). The data from MIS 1 are shown as gray lines (time axis on top) for comparison; the curves are aligned by synchronizing the two glacial-interglacial CH_4 increases. Error bars represent the 1 SD measurement uncertainty. Data are plotted on the EDC2 age scale (*3*).

MISs 13.3 and 13.1 look similar to those of the last deglaciation (*9*): CO_2 rises first, CH_4 is delayed, and CO_2 stops rising when CH_4 rises abruptly. In comparison to the last deglaciation, the CH_4 rise at 513 kyr B.P. is rather small. This may be explained by the colder interglacial temperatures that would have favored a relative increase in methanotrophy over methanogenesis, thereby contributing to lowered net CH_4 emissions in the northern extratropics and/or the subtropical and tropical regions. Additionally, the Northern Hemisphere ice sheets may not have retreated as far north during MIS 13. As a consequence, the uncovered areal extent of additional CH_4 source regions was smaller and therefore, the CH_4 overshoot, usually found at terminations, may not have occurred.

At this point, it is difficult to characterize MISs 13 and 15 as interglacials, because the δD values barely exceed –403‰. We therefore refer to these periods as intermediate warm periods (IWP) (*27*). This and their specific evolution of CH_4 suggests that they are similar to MISs 5.1 to 5.3 and MISs 7.1 to 7.3 (*2*) (Fig. 4). In all cases, regular events with CH_4 amplitudes of 50 to 140 ppbv occurred, similar to events marked by stars in Fig. 2. The average return time of the events during MIS 13 is approximately 20 ky, and they last for 5 to 10 ky. The origin of these fluctuations is probably related to the precession cycle (19 to 23 ky) of summer insolation in mid-low to low northern latitudes, as observed for the CH_4 amplitude during the last glacial period (*13*). The N_2O amplitude appears to be modulated by different mechanisms from those responsible for CH_4, as seen in MISs 13 and 15 (e.g., at 498 and 596 kyr B.P.), where N_2O peaks are quite large despite the small CH_4 peaks. Similar discrepancies are in fact found in the last glacial period, e.g., at D/O events 19 and 20 (*13*).

MIS 12 is believed to be a very cold period showing millennial time-scale variations similar to those observed in the last glacial period (*28*). The Dome C record shows CH_4 variations lasting about 1 to 3 ky, with amplitudes of 40 to 120 ppbv (Fig. 2). In addition, Antarctic warming events of 7 to 19‰ are present in the δD record. Their independent evolution on millennial time scales is an indication that the bipolar seesaw may have been operational also during MIS 12 (*29*), but the resolution of our measurements and the uncertainty in their timing prevent us from drawing final conclusions.

Our CH_4 measurements provide an undisturbed record for the entire MIS 11 (Fig. 3B) and support, except for a small offset (*19*), the recently reconstructed MIS 11 record of Vostok (*30*). This is important for two reasons. First, MIS 11 is the longest warm phase of the Antarctic temperature record over the past 740 ky (*24*), with a mean temperature comparable to the Holocene. CH_4 exceeded the minimum Holocene value of 560 ppbv for more than 28 ky. Second, CH_4 increased to 689 ppbv at termination V, followed by an early decrease for about 5000 years, which is very similar to the early Holocene CH_4 record (gray curves in Fig. 3B). It then rose to the high concentration of about 700 ppbv. Ruddiman (*31*) argued that such a behavior of the CH_4 during the early Holocene is due to early anthropogenic interference and that this would be unique. Our data provide a crucial counterexample to this postulated behavior: The early temporary reduction was clearly not an indication of an impending ice age, which started some 20,000 years later in MIS 11, and the increase after this reduction has been established without human influence.

The good agreement between the Dome C and the Vostok (*15*, *30*) record over MISs 1 to 7 and MIS 11 increases our confidence in the fidelity of a composite record of atmospheric CH_4 over the past 650 ky (Fig. 4). The composite record, established by wiggle matching (*32*), demonstrates, within the resolution of our measurements, that preindustrial atmospheric concentrations of CH_4 reconstructed from two Antarctic ice cores have not exceeded 773 ± 15 ppbv (single values at MIS 9.3) during the past 650 ky. The highest mean N_2O values (278 ppbv ± 7 ppbv) over at least a period of 7 ky covered by our records are found during MIS 15.1, slightly higher than early Holocene values. The differing response to climate change of CH_4 and N_2O during MISs 15.1 and 15.5 suggests that the main source regions and/or strengths may strongly differ during interglacials and IWP. High levels are sustained longer for N_2O than for CH_4 during MISs 5.5, 15.1, and 15.3 (Fig. 4), either due to the release of oceanic N_2O or because N_2O soil sources are also productive under semiarid conditions (*13*).

In general, CH_4 is well correlated with δD on glacial-interglacial time scales (>40 ky), including lower CH_4 concentrations during the IWP than during interglacials of the past 420 ky. At terminations, the amplitude of the CH_4 increase is highly correlated with the corresponding Antarctic temperature (r^2 = 0.80). CH_4 has mainly tropical and Northern Hemisphere sources, but only very small austral sources (mainly open-ocean contributions), which suggests that the generally smaller glacial-interglacial temperature change before 440 kyr B.P. revealed by Dome C δD was also of global importance at that time (*33*). The precessional insolation signal in low- to mid-northern latitudes has a strong influence on the amplitude of CH_4 variations for glacial periods and IWP, but the Northern wetlands, episodically covered by boreal ice sheets and exposed to different precipitation patterns, are likely to contribute to this D/O-like variability of the CH_4 concentration (*21*). Furthermore, sink feedbacks, through changes

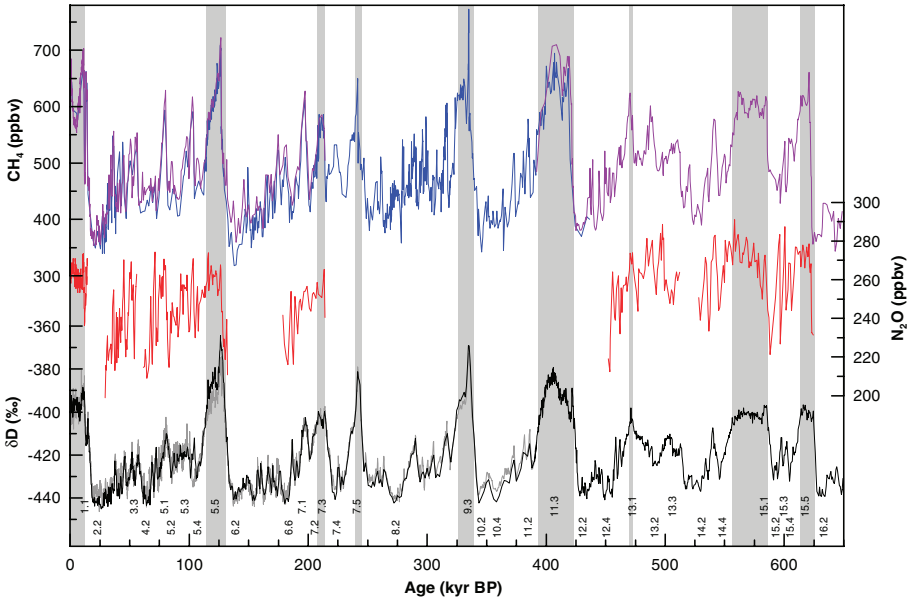

Fig. 4. CH_4 record over the past 650 ky, composed of Dome C CH_4 (purple line) [(*8*, *9*) and new data] and Vostok CH_4 (blue line) (*2*, *15*). Also shown are the N_2O data measured along the Dome C ice cores (red line) [(*8*, *20*, *36*) and new data] and δD records from Dome C (black line) (*24*) as well as those from Vostok +42‰ (gray line) (*2*). N_2O artifacts are not shown in this figure. Gray shaded areas highlight interglacial periods with a δD value >–403‰ as defined in (*3*). Numbers of MISs are given at the bottom of the figure (*25*). Data are shown on the EDC2 time scale (*3*).

of hydrocarbon emissions from the terrestrial biosphere, could have been considerable (*34*).

References and Notes

1. L. E. Lisiecki, M. E. Raymo, *Paleoceanography* **20**, PA1003 (2005).
2. J. R. Petit *et al.*, *Nature* **387**, 359 (1999).
3. EPICA Community Members, *Nature* **431**, 147 (2004).
4. T. Blunier *et al.*, *Geophys. Res. Lett.* **20**, 2219 (1993).
5. D. M. Etheridge, L. P. Steele, R. J. Francey, R. L. Langenfelds, *J. Geophys. Res.* **103**, 15979 (1998).
6. J. Flückiger *et al.*, *Science* **285**, 227 (1999).
7. J. Chappellaz *et al.*, *J. Geophys. Res.* **102**, 15987 (1997).
8. J. Flückiger *et al.*, *Global Biogeochem. Cycles* **16**, 1010 (2002).
9. E. Monnin *et al.*, *Science* **291**, 112 (2001).
10. T. Blunier *et al.*, *Nature* **394**, 739 (1998).
11. E. J. Brook, T. Sowers, J. Orchardo, *Science* **273**, 1087 (1996).
12. J. Chappellaz *et al.*, *Nature* **366**, 443 (1993).
13. J. Flückiger *et al.*, *Global Biogeochem. Cycles* **18**, GB1020 (2004).
14. T. Sowers, R. B. Alley, J. Jubenville, *Science* **301**, 945 (2003).
15. M. Delmotte *et al.*, *J. Geophys. Res.* **109**, D12104 (2004).
16. K. Kawamura, thesis, Tohoku University, Tohoku, Japan (2000).
17. T. Sowers, *J. Geophys. Res.* **106**, 31903 (2001).
18. J. Chappellaz, I. Y. Fung, A. M. Thompson, *Tellus* **45B**, 228 (1993).
19. Materials and methods are available as supporting material on *Science* Online.
20. B. Stauffer, J. Flückiger, E. Monnin, T. Nakazawa, S. Aoki, *Mem. Natl. Inst. Polar Res.* **57**, 139 (2003).
21. A. Dällenbach *et al.*, *Geophys. Res. Lett.* **27**, 1005 (2000).
22. R. Spahni *et al.*, *Geophys. Res. Lett.* **30**, 1571 (2003).
23. NorthGRIP Project Members, *Nature* **431**, 147 (2004).
24. J. Jouzel, in preparation.
25. M. Sarnthein, R. Tiedemann, *Paleoceanography* **5**, 1 (1990).
26. U. Siegenthaler *et al.*, *Science* **310**, 1313 (2005).
27. For MISs 13.1, 13.3, 15.1, and 15.5, δD barely exceeds –403‰, so we use the term intermediate warm period (IWP) for those periods with a lower δD that is still above –425‰ (minimum at MIS 13.2 in Fig. 2). This applies also to MISs 5.1, 5.3, 7.1, and 7.3.
28. D. W. Oppo, J. F. McManus, J. L. Cullen, *Science* **279**, 1335 (1998).
29. T. F. Stocker, S. J. Johnsen, *Paleoceanography* **18**, 1087 (2003).
30. D. Raynaud *et al.*, *Nature* **436**, 39 (2005).
31. W. F. Ruddiman, *Clim. Change* **61**, 261 (2003).
32. The synchronization of the Vostok to the longer Dome C record first has been wiggle matched (*35*) by δD. Then, Vostok gas ages are calculated using Vostok age A55 (*15*), refined by directly matching (*35*) CH_4 from Vostok to Dome C in overlapping periods.
33. V. Masson-Delmotte *et al.*, in preparation.
34. P. J. Valdes, D. J. Beerling, C. E. Johnson, *Geophys. Res. Lett.* **32**, L02704 (2005).
35. J. Schwander *et al.*, *J. Geophys. Res.* **102**, 19483 (1997).
36. B. Stauffer *et al.*, *Ann. Glaciol.* **35**, 202 (2002).
37. T. Blunier, E. J. Brook, *Science* **291**, 109 (2001).

38. We thank U. Siegenthaler, F. Lambert, T. Blunier, and B. Stauffer for discussions and two anonymous reviewers for their comments. This is EPICA publication no. 134. This work is a contribution to the European Project for Ice Coring in Antarctica (EPICA), a joint ESF (European Science Foundation)/European Commission (EC) scientific program, funded by the EC and by national contributions from Belgium, Denmark, France, Germany, Italy, the Netherlands, Norway, Sweden, Switzerland, and the United Kingdom. We acknowledge long-term financial support by the Swiss National Science Foundation and the Swiss Federal Office of Energy for both science and logistic contributions to EPICA and to the University of Bern. Support was also provided by the French program PNEDC (INSU-CNRS), and the EC project EPICA-MIS.

Supporting Online Material
www.sciencemag.org/cgi/content/full/310/5752/1317/DC1
Materials and Methods
Figs. S1 to S3
References

13 September 2005; accepted 2 November 2005
10.1126/science.1120132

Assistance of Microbial Glycolipid Antigen Processing by CD1e

Henri de la Salle,[1]* Sabrina Mariotti,[2]* Catherine Angenieux,[1]* Martine Gilleron,[3]* Luis-Fernando Garcia-Alles,[4] Dag Malm,[5] Thomas Berg,[6] Samantha Paoletti,[2] Blandine Maître,[1] Lionel Mourey,[4] Jean Salamero,[7] Jean Pierre Cazenave,[8] Daniel Hanau,[1] Lucia Mori,[2] Germain Puzo,[3]† Gennaro De Libero[2]†

Complexes between CD1 molecules and self or microbial glycolipids represent important immunogenic ligands for specific subsets of T cells. However, the function of one of the CD1 family members, CD1e, has yet to be determined. Here, we show that the mycobacterial antigens hexamannosylated phosphatidyl-*myo*-inositols (PIM_6) stimulate CD1b-restricted T cells only after partial digestion of the oligomannose moiety by lysosomal α-mannosidase and that soluble CD1e is required for this processing. Furthermore, recombinant CD1e was able to bind glycolipids and assist in the digestion of PIM_6. We propose that, through this form of glycolipid editing, CD1e helps expand the repertoire of glycolipidic T cell antigens to optimize antimicrobial immune responses.

Particular subsets of T cells recognize lipidic and glycolipidic antigens presented by CD1a, b, c, or d proteins, which are antigen-presenting molecules structurally similar to major histocompatibility complex (MHC) class I proteins (*1*). However, unlike classical MHC molecules, CD1 proteins are functionally nonpolymorphic and expressed in a restricted number of cell types, including myeloid dendritic cells (DCs) (*2*). Each CD1 isotype can be characterized by a distinct intracellular trafficking pathway, which allows the capture of lipid antigens either in late or early endosomal compartments (*2*). In particular, CD1b binds glycolipid antigens in MHC class II–enriched lysosomes (*3*) and returns to the plasma membrane to stimulate antigen-specific T cells.

CD1-presented lipid antigens can be of self (*4–7*) or microbial (*8–14*) origin and can include one or more acyl appendages that anchor into the hydrophobic pockets of CD1 protein, as well as a polar moiety directed out toward the T cell receptor (TCR). Exposed amino acids present in α helices of CD1 molecules, together with polar groups of the antigen, directly interact with the TCR and thus constrain the space between CD1 and TCR (*7*, *12*, *15*, *16*). Because such constraint is likely to prevent accommodation and recognition of antigens with large polar heads, it is generally accepted that antigenic glycolipids and lipoglycans with large oligosaccharide moieties are first processed so that T cell recognition can take place.

Relatively little is known about the molecular mechanisms of glycolipid processing. However, previous work has demonstrated that, to be recognized, the oligosaccharide moiety of Gal(α1→2)GalCer must first be cleaved by the lysosomal α-galactosidase (*17*) in the presence of lipid transfer proteins (LTPs) known as saposins, which are involved in the catabolism of endogenous glycolipids (*18*).

Some species express a particular CD1 isoform, CD1e, which has remained the only member of this protein family with undetermined function. CD1e molecules mainly localize within Golgi compartments of

[1]INSERM, U725, Etablissement Francais du Sang-Alsace, F-67065 Strasbourg, France. [2]Experimental Immunology, Department of Research, Basel University Hospital, CH-4031 Basel, Switzerland. [3]CNRS, UMR 5089, Immunochimie et Glycoconjugués Mycobacteriens, and [4]Biophysique Structurale, Département Mécanismes Moléculaires des Infections Mycobactériennes, Institut de Pharmacologie et de Biologie Structurale, F-31077 Toulouse Cedex, France. [5]Department of Medicine and [6]Department of Pathology, University Hospital of Northern Norway, N-9038 Tromsø, Norway. [7]CNRS, UMR 144, Institut Curie, F-75005 Paris, France. [8]INSERM, U311, Etablissement Francais du Sang-Alsace, F-67065 Strasbourg, France.

*These authors contributed equally to this work.
†To whom correspondence should be addressed. E-mail: gennaro.delibero@unibas.ch (G.D.L.); germain.puzo@ipbs.fr (G.P.)